Nano Research
2019, 12(7): 1631–1634

ISSN 1998-0124 CN 11-5974/O4
https://doi.org/10.1007/s12274-019-2411-y

Research Article

Selective hydrogenation of N-heterocyclic compounds over rhodium-copper bimetallic nanocrystals under ambient conditions

Muhammad Mateen, Khadim Shah, Zheng Chen (✉), Chen Chen, and Yadong Li

Department of Chemistry, Tsinghua University, Beijing 100084, China

Received: 29 January 2019 / **Revised:** 25 March 2019 / **Accepted:** 8 April 2019

ABSTRACT

Bimetallic nanocrystals (BMNCs) with distinguished electronic and chemical properties from those of their parent metals, offer the opportunity to obtain new catalysts with enhanced selectivity, activity, and stability. Here we describe the facile synthesis of rhodium-copper bimetallic system with different compositions and uniform morphology for chemo selective hydrogenation of functionalized quinolines. Our findings demonstrate that Rh-Cu BMNCs exhibited composition dependent activity and selectivity. BMNCs with rhodium to copper ratio 3:1 surpassed individual Rh and Cu and other compositions both in activity and selectivity for quinolines hydrogenation and performed even better than Rh/C with same amount of Rh. Rh_3Cu_1 catalyst displayed excellent tolerance for synthetically significant functional groups such as –OH, NH_2, F, particularly for aldehyde group which is very reactive towards reduction. These results suggested that the coexistence of rhodium and copper metals play important role in the enhancement of catalytic activity due to synergistic effects and revealed that bimetallic nanocrystals can be promising as practical catalysts for selective hydrogenation of quinoline and other substrates.

KEYWORDS

bimetallic, nanocrystals, N-heterocycles, selective hydrogenation, rhodium-copper

Selective hydrogenation of N-heterocyclic compounds, such as quinolines is important transformation because of their application in pharmaceuticals and other biologically active products [1–3]. Most straightforward way in term of simplicity and efficiency is the regio-selective hydrogenation of readily available quinolines to tetrahydroquinolines [4]. However, the direct hydrogenation of quinolines molecules with high selectivity and atomic economy is extremely difficult due to the aromatic nature of the quinoline ring and poisoning of the catalysts [5, 6]. Recently, numbers of homogeneous and heterogeneous systems based on traditional noble metals (Pd, Pt, Ru, Rh, etc.) have been developed for selective hydrogenation [7–12]. These systems suffer from inherent problems associated with catalyst reusability, use of co-catalysts and strongly absorbed quinolines and/or their hydrogenated derivatives on catalysts surface [13]. Unfortunately, most of the catalysts reported to date for quinolines conversion to tetrahydroquinolines require either high temperature or pressure. For instant hydrogenation of quinolines is carried out over Ir catalyst at room temperature and 15 atm [14]. Therefore, search for novel and efficient catalysts that can facilitate selective quinoline hydrogenation under mild and ligand-free conditions remains a challenging but rewarding task.

Bimetallic nanocrystals have received great consideration for their architectural diversity and distinguished characteristics [15]. The development of bimetallic nanocrystals is an enduring research area in heterogeneous catalysis. So far, a number of bimetallic catalysts have been synthesized and explored by many groups for a variety of chemical transformations in industrial chemistry, selective oxidation and hydrogenation, coupling reactions and electro-catalysis [16–25]. Although bimetallic catalysts are more complex regarding synthesis and structure characterization, still they are superior in many aspects. First, the incorporation of metals such as Cu, into the precious metals (Pt, Rh, Pd, Ir) which are widely used in heterogeneous catalysis can reduce the cost of materials. Secondly, the tuning of physical, and chemical properties of bimetallic nanoparticles through surface composition, size and structure, can lead to promising catalysts with enhanced activity and selectivity towards desire product [26, 27]. Rh nanocrystals find extensive application in hydrogenation reactions especially for compounds with aromatic rings [28–30]. The outstanding hydrogen dissociation capacity of Rh metal can lead to excessive hydrogenation, which makes it difficult for Rh to control the hydrogenation selectivity of compounds with reducible functional groups. The introduction of exotic metals to Rh nanoparticles not only reduces the usage of rhodium, but also shows superior catalytic performance to pure Rh catalysts in some catalytic reactions [31, 32]. However, Rh-based bimetallic catalysts have rarely been explored for quinolines hydrogenation reactions.

Herein we report well controlled protocol for the synthesis of RhCu bimetallic nanocrystals with various Rh to Cu ratio. Typically, poly dispersed nanocrystals are obtained by conventional synthetic methods. Our approach yielded highly mono dispersed nanocrystals with various compositions. The composition of Rh-Cu BMNCs was controlled by changing the Rh to Cu precursor molar ratios. Detail experimental procedure is given in the Electronic Supplementary Material (ESM). As prepared bimetallic nanocrystals were characterized by X-ray diffraction (XRD), transmission electron microscopy (TEM), high angular annular dark-field scanning transmission electron microscopy (HAADF-STEM) and X-ray photoelectron spectroscopy (XPS) to reveal the crystal structure, morphology, composition, and local atomic structure of the BMNCs. Bimetallic RhCu nanocatalysts were investigated for the selective hydrogenation of substituted

Address correspondence to chenlcao@mail.tsinghua.edu.cn or chenxzheng@126.com

quinolines at ambient temperature. RhCu BMNCs exhibited composition dependent catalytic activities and selectivity for broad substrate range with excellent functional group tolerance.

TEM images of bimetallic nanoparticles with different stoichiometric ratio along with pure Rh and Cu nanocrystals are presented in Figs. 1(a)–1(d) and Fig. S2 in the ESM. All the RhCu BMNCs exhibits good dispersion and narrow size distribution as evident from TEM images. Powder XRD pattern of the as-synthesized nanocrystals with different Rh, Cu contents along with monometallic Rh and Cu nanoparticles is given in Fig. S1 in the ESM. The shift and shortening of the Rh diffraction peak at 40.6° (2θ) toward higher angles with increasing Cu contents resulted from substitution of Cu atoms for Rh atoms clearly demonstrate the formation of the bimetallic structure.

XPS of Rh_3Cu_1 nanocrystals confirmed the coexistence of metallic Rh and Cu Figs. 2(d) and 2(e). According to the XPS, the Cu/Rh atomic ratio is 1/2.87 for Rh_3Cu_1 which is inconsistence with the results obtained from the ICP-OES. XPS spectra of Rh in Rh_3Cu_1 exhibited binding energies peaks for Rh $3d_{5/2}$ and Rh $3d_{3/2}$ at 307.47 and 312.28 eV respectively in Fig. 2(d). These peaks slightly shifted to lower energy side relative to monometallic Rh can be assigned to Rh(0) [33]. XPS peaks analysis of Rh suggest that Rh is predominantly present in zero valence state, which is similar to the reported result [34]. The binding energy peak at 932.4 eV of Cu $2p_{3/2}$ XPS spectra can be attributed to Cu^0 or Cu^+ which are on lower energy values for Rh_3Cu_1 (Fig. 2(e)). However binding energy of Cu^0 and Cu^+ species can overlap in Cu 2p XPS spectra, but could be distinguished by their different kinetic energies in the Cu LMM XAES spectra. The broad and asymmetric Cu LMM XAES spectra (inset of Fig. 2(e)) suggest that Cu exists in at least two kinds of surface copper specie Cu^0-Cu^+ [35, 36].

HAADF-STEM and energy-dispersive X-ray spectroscopy (EDX) line scanning analysis results are given in Figs. 2(a)–2(c). EDX elemental mapping of Rh_3Cu_1 shows that Rh and Cu are uniformly distributed throughout the whole BMNCs (Fig. 2(a)). The high-resolution TEM (HRTEM) image of Rh_3Cu_1 (Fig. 2(b)) shows the lattice fringes with an inter-fringe distance of 0.216 nm for Rh_3Cu_1 which is between the characteristic face centered cubic Cu and Rh indicating the successful formation Rh-Cu bimetallic nanocrystals. Similarly, compositional line scanning profile verified the coexistence

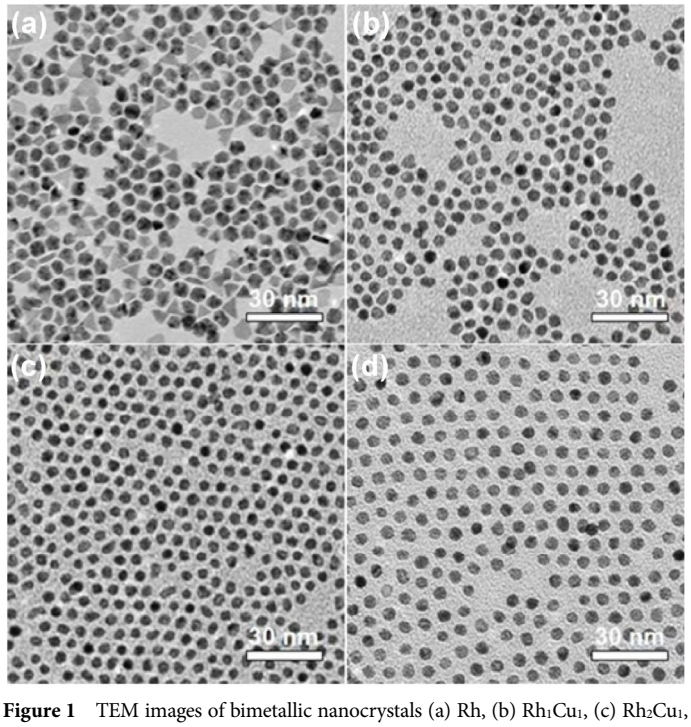

Figure 1 TEM images of bimetallic nanocrystals (a) Rh, (b) Rh_1Cu_1, (c) Rh_2Cu_1, and (d) Rh_3Cu_1

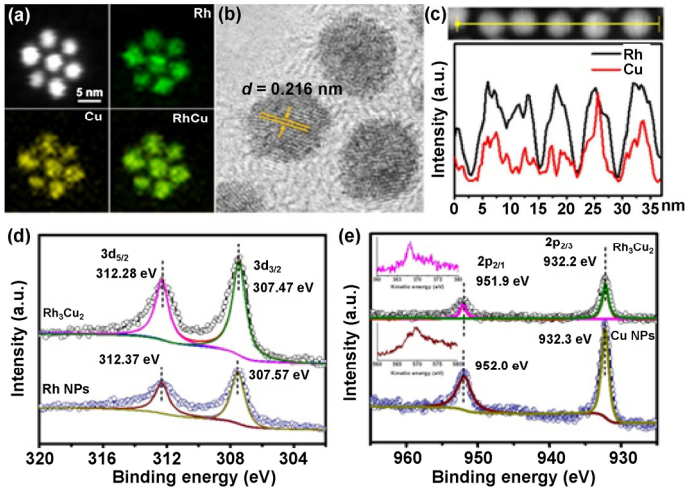

Figure 2 HAADF-STEM image (a) and EDX elemental mapping (b) of Rh_3Cu_1 nanocrystals lattice fring spacing. (c) Cross-sectional compositional line profiles of a Rh_3Cu_1 NCs. (d) XPS Rh 3d spectra of Rh_3Cu_1 and Rh NCs. (e) XPS Cu 2p spectra of Rh_3Cu_1 and Cu NCs. The insets in (e) are Auger Cu LMM spectra.

of Rh and Cu as well as the bimetallic nature of the nanocrystals (Fig. 2(c)).

After Rh_3Cu_1 nanocrystals were fully characterized we explored selective hydrogenation of quinolines as model reaction under optimized conditions to assess the catalytic performance. RhCu BMNCs with different Rh to Cu compositions were evaluated for hydrogenation along with commercial Rh/C for comparison. Reactions were performed at room temperature using H_2 gas as hydrogen source, 65 mL (0.5 mmol) of substrates and 1 mmol% of catalysts based on metals were used for evaluating the catalytic performance. The commercially available Rh/C (5 wt.%) was initially used for the quinoline hydrogenation reaction, and complete conversion was obtained after 12-h reaction time. However, ultra-high catalytic hydrogenation capacity of Rh nanoparticles results in the hydrogenation of pyridine and benzene rings of quinoline molecules simultaneously (**4** of Fig. 3(a)). The monometallic Rh nanocrystals synthesized by our method show superior selectivity towards 1,2,3,4-tetrahydroquinoline (**2** of Fig. 3(a)) but poor conversion (39.5%). Due to the irregularity in morphology and nonuniform size, the monometallic Rh nanocyrstals show inferior hydrogenation activity when compared with commercial Rh/C which is smaller and more uniform in size. Significant improvement in catalytic performance of Rh was observed on incorporation of Cu to form RhCu BMNCs. The results showing the influence of composition of the as-prepared catalysts on quinoline conversion and product selectivity are presented in Fig. 3(b). Excellent selectivity was demonstrated by all RhCu compositions towards 1,2,3,4-tetrahydroquinoline, however activity drastically varies with changing the Rh and Cu composition. Marked catalytic performance was achieved with Rh-Cu having molar ratio 3:1 (99% quinoline conversion and 98% selectivity). Improvement in catalytic activity can be attributed to synergy effect between the Rh and Cu metals. The decrease in conversion with increasing the ratio of Cu, and no activity was observed for Rh/Cu ratio less than 1:2. The monometallic Cu nanocrystals can not accomplish the dissociation of molecular hydrogen at room temperature, therefore the loss of activity emerges when using RhCu BMNCs with high ratio of Cu. These results clearly manifest that promising catalysts can be developed by simply tuning the composition of BMNCs which can be expected to have excellent activities for hydrogenation reaction. The zero-valence state of Rh makes it capable of specific adsorption of aromatic rings and dissociating hydrogen. The addition of appropriate amount of copper may induce the selective adsorption of pyridine rings, therefore

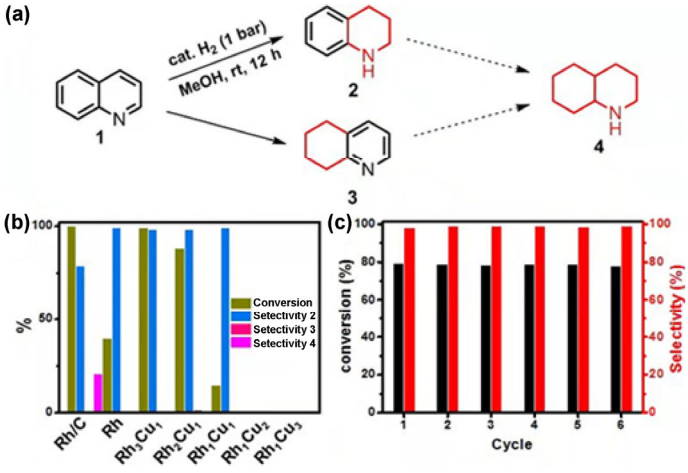

Figure 3 (a) Hydrogenated products of quinolines over Rh_3Cu nanocrystals. Substrate; 65 mL (0.5 mmol), catalyst (1 mmol% based on metal): 10 mg. (b) Conversion and selectivity of different catalysts. (c) Durability of Rh_3Cu_1 nanocrystals for six consecutive cycles.

higher activity and selectivity can be obtained.

Durability of Rh_3Cu catalyst was tested by using quinoline as substrate under optimized conditions. After completion of reaction catalyst was separated by centrifuge dried and reused for multiple times. The recycle experiments were executed at room temperature with 6 h as reaction time (Fig. 3(c)). Rh_3Cu_1 exhibited the same activity and selectivity in each repeated cycle and no decline in activity was found after six cycles, which demonstrate the excellent performance and stability. As evident from the TEM images (Fig. S3 in the ESM) there is no change in particle size and no aggregation of particles is observed after testing Rh_3Cu for six times for quinolones hydrogenation, which clearly suggest that Rh_3Cu particles are highly stable.

After screening the best RhCu BMNCs we further validated scope of Rh_3Cu_1 bimetallic catalyst with different quinolines derivatives as depicted in Table 1. Substituted quinolines derivatives both with electron donating (Table 1, entries 1–4) and electron withdrawing groups (Table 1, entries 5–9) reacted regio-selectively and only reduction of the heteroarene ring was observed. The functional group tolerance of the catalyst was studied using some particularly challenging substrates with different functional groups grafted on different parts of the quinoline structure. Chloro and flouro-substituted quinolines gave the corresponding hydrogenated products in 92% and 96% yield respectively (Table 1, entries 5 and 6). Notably, reductive dehalogenation was not observed. Remarkably, aldehyde-substituted quinolines which are considered to be much more reactive towards reduction reacted chemo-selectively and afforded the corresponding product in good conversion with excellent selectivity (Table 1, entry 10). The above observations point out that the co-existence of metallic Rh and Cu plays an important role in the significant improvement of catalytic performance and selectivity. Intermetallic electronic interactions would lead to a modification of Rh electronic structure and exert a considerable effect on adjustment of the bonding pattern between catalyst surface and reactants, as well as the stability of the reaction intermediate.

Finally, we carried out the hydrogenation of quinolines at selected temperatures (25, 35, and 45 °C). The effect of temperature on quinoline transformation rate is studied by using Arrhenius plots (Fig. S4 in the ESM). Activation energy calculated from slopes of Arrhenius plots decreases with increase in temperatures (Fig. S4(b) in the ESM). The activation energy for quinoline calculated from Arrhenius plots at 45 °C is 28.4 kJ/mol.

In conclusion, we reported the preparation of highly active, selective and recyclable Rh_3Cu_1 nanocatalysts for selective hydrogenation of

Table 1 The scope of quinolines hydrogenation catalyzed by Rh_3Cu_1 bimetallic catalyst

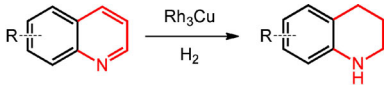

Entry[a]	Substrate	Product	Con./Sel. (%)[b]
1			97.1/98.2
2		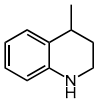	96.5/97.1
3	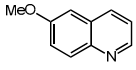	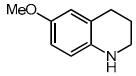	96.3/96.1
4	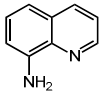	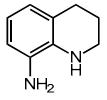	90.3/97.7
5	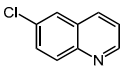	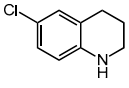	92.3/97.6
6	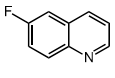	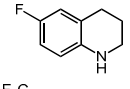	88.7/96.5
7	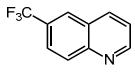	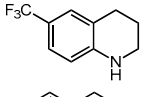	90.6/98.9
8	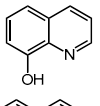	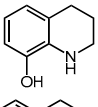	86.2/97.3
9	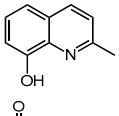	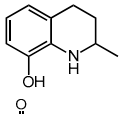	96.1/97.1
10	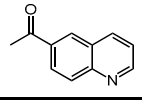	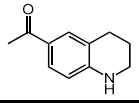	92.3/97.6

[a]Reaction conditions: 0.5 mmol substrate, 10 mg catalyst, 3 mL MeOH, rt, 12 h. [b]The yields are determined by GC analysis.

quinolines bearing some challenging functional groups which are more susceptible to hydrogenation. Our findings demonstrated that combination of a non-noble and noble metal with optimized composition can result in enhancement of activity and improvement of selectivity. The high activity and selectivity of Rh_3Cu_1 bimetallic nanocrystals point out their potentials for practical applications and reduce the cost of expensive noble metals based catalysts.

Acknowledgements

This work was supported by the National Key R&D Program of China (Nos. 2016YFA0202801 and 2017YFA0700101), the National Natural Science Foundation of China (Nos. 21573119, 21590792, 21890383, and 21872076), and China Postdoctoral Science Foundation (No. 2018M631444).

Electronic Supplementary Material: Supplementary material is available in the online version of this article at https://doi.org/10.1007/s12274-019-2411-y.

References

[1] Ren, D.; He, L.; Yu, L.; Ding, R. S.; Liu, Y. M.; Cao, Y.; He, H. Y.; Fan, K. N. An unusual chemoselective hydrogenation of quinoline compounds using supported gold catalysts. *J. Am. Chem. Soc.* **2012**, *134*, 17592–17598.

[2] Sridharan, V.; Suryavanshi, P. A.; Menéndez, J. C. Advances in the chemistry of tetrahydroquinolines. *Chem. Rev.* **2011**, *111*, 7157–7259.

[3] Shahane, S.; Louafi, F.; Moreau, J.; Hurvois, J. P.; Renaud, J. L.; van de Weghe, P.; Roisnel, T. Synthesis of alkaloids of *Galipea officinalis* by alkylation of an α-amino nitrile. *Eur. J. Org. Chem.* **2008**, *2008*, 4622–4631.

[4] Pitts, M. R.; Harrison, J. R.; Moody, C. J. Indium metal as a reducing agent in organic synthesis. *J. Chem. Soc. Perkin Trans. 1*. **2001**, 955–977.

[5] Wang, D. S.; Chen, Q. A.; Lu, S. M.; Zhou, Y. G. Asymmetric hydrogenation of heteroarenes and arenes. *Chem. Rev.* **2012**, *112*, 2557–2590.

[6] Karakulina, A.; Gopakumar, A.; Akçok, İ.; Roulier, B. L.; LaGrange, T.; Katsyuba, S. A.; Das, S.; Dyson, P. J. A rhodium nanoparticle–lewis acidic ionic liquid catalyst for the chemoselective reduction of heteroarenes. *Angew. Chem., Int. Ed.* **2016**, *55*, 292–296.

[7] Ren, Y.; Wang, Y.; Li, X.; Zhang, Z.; Chi, Q. Selective hydrogenation of quinolines into 1,2,3,4-tetrahydroquinolines over a nitrogen doped carbon-supported Pd catalyst. *New J. Chem.* **2018**, *42*, 16694–16702.

[8] Wang, C.; Li, C. Q.; Wu, X. F.; Pettman, A.; Xiao, J. L. pH-regulated asymmetric transfer hydrogenation of quinolines in water. *Angew. Chem., Int. Ed.* **2009**, *48*, 6524–6528.

[9] Zhao, M. T.; Yuan, K.; Wang, Y.; Li, G. D.; Guo, J.; Gu, L.; Hu, W. P.; Zhao, H. J.; Tang, Z. Y. Metal-organic frameworks as selectivity regulators for hydrogenation reactions. *Nature* **2016**, *539*, 76–80.

[10] Zhao, M. T.; Deng, K.; He, L. C.; Liu, Y.; Li, G. D.; Zhao, H. J.; Tang, Z. Y. Core-shell palladium nanoparticle@metal-organic frameworks as multifunctional catalysts for cascade reactions. *J. Am. Chem. Soc.* **2014**, *136*, 1738–1741.

[11] Schlögl, R. Heterogeneous catalysis. *Angew. Chem., Int. Ed.* **2015**, *54*, 3465–3520.

[12] Chen, Y. G.; Yu, Z. J.; Chen, Z.; Shen, R. A.; Wang, Y.; Cao, X.; Peng, Q.; Li, Y. D. Controlled one-pot synthesis of RuCu nanocages and Cu@Ru nanocrystals for the regioselective hydrogenation of quinoline. *Nano Res.* **2016**, *9*, 2632–2640.

[13] Hashimoto, N.; Takahashi, Y.; Hara, T.; Shimazu, S.; Mitsudome, T.; Mizugaki, T.; Jitsukawa, K.; Kaneda, K. Fine tuning of Pd^0 nanoparticle formation on hydroxyapatite and its application for regioselective quinoline hydrogenation. *Chem. Lett.* **2010**, *39*, 832–834.

[14] Dobereiner, G. E.; Nova, A.; Schley, N. D.; Hazari, N.; Miller, S. J.; Eisenstein, O.; Crabtree, R. H. Iridium-catalyzed hydrogenation of N-heterocyclic compounds under mild conditions by an outer-sphere pathway. *J. Am. Chem. Soc.* **2011**, *133*, 7547–7562.

[15] Yu, W. T.; Porosoff, M. D.; Chen, J. G. Review of Pt-based bimetallic catalysis: From model surfaces to supported catalysts. *Chem. Rev.* **2012**, *112*, 5780−5817.

[16] Liu, Y.; Chi, M. F.; Mazumder, V.; More, K. L.; Soled, S.; Henao, J. D.; Sun, S. H. Composition-controlled synthesis of bimetallic PdPt nanoparticles and their electro-oxidation of methanol. *Chem. Mater.* **2011,** *23*, 4199−4203.

[17] Xiang, J.; Li, P.; Chong, H. B.; Feng, L.; Fu, F. Y.; Wang, Z.; Zhang, S. L.; Zhu, M. Z. Bimetallic Pd–Ni core–shell nanoparticles as effective catalysts for the Suzuki reaction. *Nano Res.* **2014**, *7*, 1337–1343.

[18] Wang, Y. H.; Li, L. D.; Wu, K.; Si, R.; Sun, L. D.; Yan, C. H. Composition-tuned oxidation levels of Pt–Re bimetallic nanoparticles for the etherification of allylic alcohols. *Nano Res.* **2018**, *11*, 5902–5912.

[19] Ahmadi, M.; Behafarid, F.; Cui, C. H.; Strasser, P.; Cuenya, B. R. Long-range segregation phenomena in shape-selected bimetallic nanoparticles: Chemical state effects. *ACS Nano* **2013**, *7*, 9195−9204.

[20] Wang, W. Y.; Wang, D. S.; Liu, X. W.; Peng, Q.; Li, Y. D. Pt-Ni nanodendrites with high hydrogenation activity. *Chem. Commun.* **2013,** *49*, 2903−2905.

[21] Ye, W.; Kou, S. F.; Guo, X.; Xie, F.; Sun, H. Y.; Lu, H. T.; Yang, J. Controlled synthesis of bimetallic Pd-Rh nanoframes and nanoboxes with high catalytic performances. *Nanoscale* **2015**, *7*, 9558−9562.

[22] Xia, B. Q.; Chen, K.; Luo, W.; Cheng, G. Z. NiRh nanoparticles supported on nitrogen-doped porous carbon as highly efficient catalysts for dehydrogenation of hydrazine in alkaline solution. *Nano Res.* **2015**, *8*, 3472–3479.

[23] Zhu, W.; Shan, J. J.; Nguyen, L.; Zhang S. R.; Tao, F. F.; Zhang, Y. W. Evolution of surface of Pd-Rh bimetallic nanocubes and its correlation with CO oxidation. *Sci. China Mater.* **2019**, *62*, 103–114.

[24] Furukawa, S.; Takahashi, K.; Komatsu, T. Well-structured bimetallic surface capable of molecular recognition for chemoselective nitroarene hydrogenation. *Chem. Sci.* **2016**, *7*, 4476–4484.

[25] Chen, C.; Kang, Y. J.; Huo, Z. Y.; Zhu, Z. W.; Huang, W. Y.; Xin, H. L.; Snyder, J. D.; Li, D. G.; Herron, J. A.; Mavrikakis, M. et al. Highly crystalline multimetallic nanoframes with three-dimensional electrocatalytic surfaces. *Science* **2014**, *343*, 1339–1343.

[26] Gilroy, K. D.; Ruditskiy, A.; Peng, H. C.; Qin, D.; Xia Y. N. Bimetallic nanocrystals: Syntheses, properties, and applications. *Chem. Rev.* **2016**, *116*, 10414−10472.

[27] Mao, J. J.; Liu, Y. X.; Chen, Z.; Wang, D. S.; Li, Y. D. Bimetallic Pd–Cu nanocrystals and their tunable catalytic properties. *Chem. Commun.* **2014**, *50*, 4588–4591.

[28] Fan, G. Y.; Wu, J. Mild hydrogenation of quinoline to decahydroquinoline over rhodium nanoparticles entrapped in aluminum oxy-hydroxide. *Catal. Commun.* **2013**, *31*, 81–85.

[29] Campanati, M.; Vaccari, A.; Piccolo, O. Mild hydrogenation of quinoline: 1. Role of reaction parameters. *J. Mol. Catal. A- Chem.* **2002**, *179*, 287–292.

[30] Sánchez, A.; Fang, M. F.; Ahmed, A.; Sánchez-Delgado, R. A. Hydrogenation of arenes, N-heteroaromatic compounds, and alkenes catalyzed by rhodium nanoparticles supported on magnesium oxide. *Appl. Catal. A Gen.* **2014**, *477*, 117–124.

[31] Sharif, Md. J.; Yamazoe, S.: Tsukuda, T. Selective hydrogenation of 4-nitrobenzaldehyde to 4-aminobenzaldehyde by colloidal RhCu bimetallic nanoparticles. *Top. Catal.* **2014**, *57*, 1049–1053.

[32] Park, J.; Kim, J.; Yang, Y.; Yoon, D.; Baik, H.; Haam, S.; Yang, H.; Lee, K. RhCu 3D nanoframe as a highly active electrocatalyst for oxygen evolution reaction under alkaline condition. *Adv. Sci.* **2016**, *3*, 1500252

[33] Lin, J.; Chen, J.; Su, W. P. Rhodium-cobalt bimetallic nanoparticles: A catalyst for selective hydrogenation of unsaturated carbon-carbon bonds with hydrous hydrazine. *Adv. Synth. Catal.* **2013**, *355*, 41–46.

[34] Jiang, B.; Kani, K.; Iqbal, M.; Abe, H.; Kimura, T.; Hossain, M. S. A.; Anjaneyulu, O.; Henzie, J.; Yamauchi, Y. Mesoporous bimetallic RhCu alloy nanospheres using a sophisticated soft-templating strategy. *Chem. Mater.* **2018**, *30*, 428–435.

[35] Espinós, J. P.; Morales, J.; Barranco, A.; Caballero, A.; Holgado, J. P.; González-Elipe, A. R. Interface effects for Cu, CuO, and Cu_2O deposited on SiO_2 and ZrO_2. XPS Determination of the valence state of copper in Cu/SiO_2 and Cu/ZrO_2 catalysts. *J. Phys. Chem. B.* **2002**, *106*, 6921−6929.

[36] Yin, A. Y.; Guo, X. Y.; Dai, W. L.; Fan, K. N. The nature of active copper species in Cu-HMS catalyst for hydrogenation of dimethyl oxalate to ethylene glycol: New insights on the synergetic effect between Cu^0 and Cu^+. *J. Phys. Chem. C.* **2009**, *113*, 11003−11013.